LETTERS

Active turnover modulates mature microRNA activity in *Caenorhabditis elegans*

Saibal Chatterjee[1] & Helge Großhans[1]

MicroRNAs (miRNAs) constitute a large class of regulatory RNAs that repress target messenger RNAs to control various biological processes[1]. Accordingly, miRNA biogenesis is highly regulated, controlled at both transcriptional and post-transcriptional levels[2], and overexpression and underexpression of miRNAs are linked to various human diseases, particularly cancers[1,3]. As RNA concentrations are generally a function of biogenesis and turnover, active miRNA degradation might also modulate miRNA accumulation, and the plant 3′→5′ exonuclease SDN1 has been implicated in miRNA turnover[4]. Here we report that degradation of mature miRNAs in the nematode *Caenorhabditis elegans*, mediated by the 5′→3′ exoribonuclease XRN-2, affects functional miRNA homeostasis *in vivo*. We recapitulate XRN-2-dependent miRNA turnover in larval lysates, where processing of precursor-miRNA (pre-miRNA) by Dicer, unannealing of the miRNA duplex and loading of the mature miRNA into the Argonaute protein of the miRNA-induced silencing complex (miRISC) are coupled processes that precede degradation of the mature miRNA. Although Argonaute:miRNA complexes are highly resistant to salt, larval lysate promotes efficient release of the miRNA, exposing it to degradation by XRN-2. Release and degradation can both be blocked by the addition of miRNA target RNA. Our results therefore suggest the presence of an additional layer of regulation of animal miRNA activity that might be important for rapid changes of miRNA expression profiles during developmental transitions and for the maintenance of steady-state concentrations of miRNAs. This pathway might represent a potential target for therapeutic intervention on miRNA expression.

To identify and characterize an animal miRNA turnover pathway (Supplementary Fig. 1), we used the *let-7* miRNA as a model. *let-7* regulates cell fates in animals, and functions as a human tumour suppressor gene[5]. In *C. elegans*, the temperature-sensitive *let-7(n2853)* allele[6] causes vulval bursting at the larval-to-adult transition when animals are grown at 25 °C. A point mutation in the mature miRNA impairs its binding to target mRNAs[6,7], and the level of the mutant miRNA is moderately decreased[6,8] (Supplementary Fig. 2). Because decreased abundance seems to be functionally relevant[7], we speculated that increased abundance of the mutant *let-7* and/or its 'sister' miRNAs *mir-48*, *mir-84* and *mir-241* (ref. 9) might suffice to downregulate some targets and partly suppress vulval bursting of *let-7(n2853)* animals. We examined diverse nucleases for their ability to suppress *let-7(n2853)*-associated lethality when depleted through RNA-mediated interference (RNAi) by feeding, initiated on synchronized L1 stage larvae. *xrn-2*, the orthologue of the yeast 5′→3′ exoribonuclease Rat1p, potently suppressed vulval bursting, with more than 95% of animals surviving (Supplementary Figs 3 and 4, Supplementary Table 1 and Supplementary Text). By contrast, depletion of the *eri-1* ribonuclease, which degrades small interfering RNAs[10], or *C. elegans* homologues of *Arabidopsis SDN1* (ref. 4), did not suppress *let-7(n2853)* (Supplementary Table 1).

When we examined RNA from L4-stage *let-7(n2853)* worms, northern blotting revealed that *xrn-2(RNAi)* increased mature *let-7* levels relative to mock (empty vector) or *xrn-1(RNAi)* (Fig. 1a). This supports a role of XRN-2 in determining mutant *let-7* RNA accumulation.

Yeast Xrn2p/Rat1p performs transfer-RNA quality control, selectively removing incompletely modified tRNAs[11]. However, the effects of depletion of *C. elegans xrn-2* extended to wild-type *let-7* and unrelated miRNAs (Fig. 1a and Supplementary Fig. 5), supporting a broad function of XRN-2 in miRNA homeostasis. Overexpression of *let-7* from a transgene[12] was modestly enhanced by *xrn-2(RNAi)* at an early stage (L3), but not at later developmental stages when transgene expression was already very high (Supplementary Fig. 6), suggesting that additional homeostatic mechanisms might curtail miRNA overexpression.

The *Arabidopsis* Xrn2p/Rat1p homologues XRN2 and XRN3 degrade the loop sequence of miRNA precursors without affecting levels of mature miRNAs[13]. To investigate whether *C. elegans* XRN-2 processed pre-miRNAs, we examined the abundant pre-*mir-60* (ref. 14). Pre-*mir-60* levels were unaltered by *xrn-2* depletion, whereas mature *mir-60* accumulated (Fig. 1b). Moreover, although depletion of the pre-miRNA processing enzyme Dicer (DCR-1)[15,16] caused the accumulation of various low-abundance pre-miRNAs, *xrn-2(RNAi)* did not (Supplementary Fig. 5). Real-time polymerase chain reaction after reverse transcription (RT–qPCR) further revealed that the levels of the primary *let-7* (pri-*let-7*) and pri-*mir-77* transcripts remained unchanged on *xrn-2(RNAi)* (Fig. 1c). Thus, *xrn-2* preferentially, possibly exclusively, affects the accumulation of mature miRNAs. To our knowledge, this is the first example of XRN-2 functioning in the turnover of mature, fully functional RNA species.

To eliminate the possibility that XRN-2 simply cleared away inactive miRNAs instead of terminating miRNA activity, we examined the levels of *daf-12* and *lin-41* mRNAs, two *let-7* targets (refs 17, 18) that accumulate when *let-7* activity is lost[8,19]. Depletion of *xrn-2* in *let-7(n2853)* worms decreased the abundance of *daf-12* and *lin-41* to wild-type levels (Fig. 1d), revealing a molecular basis for suppression of *let-7(n2853)* by *xrn-2(RNAi)*. Thus, XRN-2 modulates *let-7* activity, rather than acting as a 'scavenger' enzyme.

To examine miRNA turnover biochemically, we developed an *in vitro* system using larval lysates and radiolabelled miRNAs. Initially, 3′-pCp-labelling or biotinylation were used to block the 3′ end of *let-7* against 3′→5′ exonucleolysis. Wild-type worm lysate converted these substrates to mononucleotides without the production of any visible intermediates at both 25 °C, the physiological temperature, and 37 °C (Fig. 1e and Supplementary Fig. 7). Because the latter temperature yielded more product, and for technical convenience, we performed subsequent reactions at 37 °C.

A 5′-labelled synthetic *let-7* and an internally labelled *let-7 in vitro* transcript having free 3′-hydroxyl groups were similarly degraded when exposed to the lysate (Supplementary Fig. 8a, b). Thin-layer chromatography identified the product as nucleotide 5′-monophosphate

[1]Friedrich Miescher Institute for Biomedical Research, PO Box 2543, CH-4002 Basel, Switzerland.

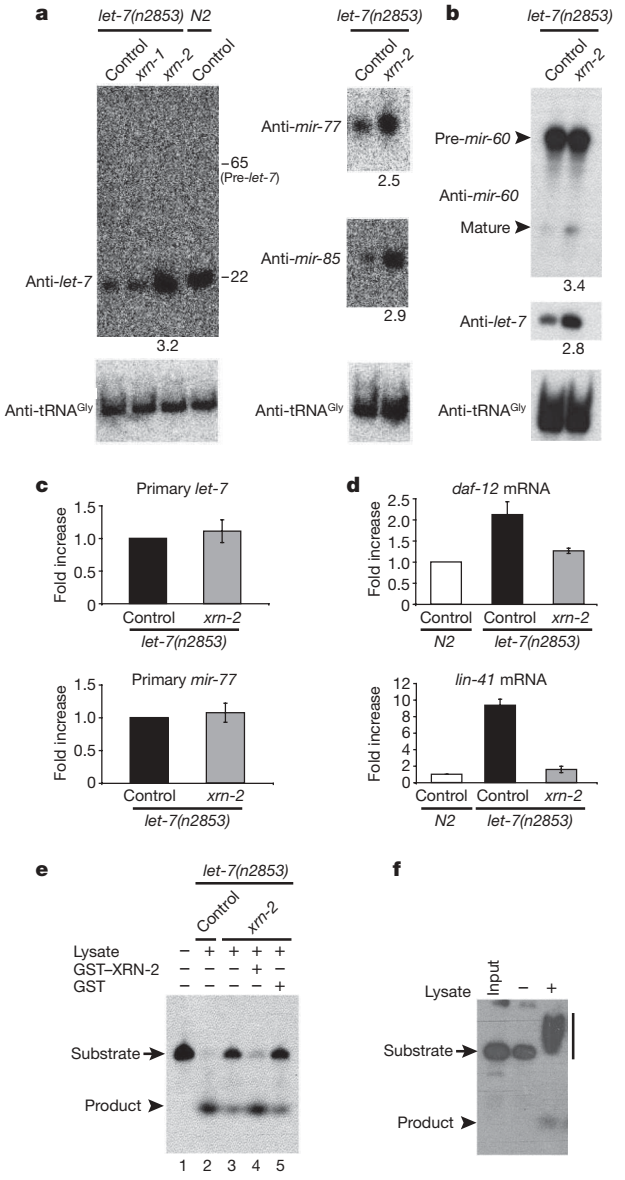

Figure 1 | Depletion of *xrn-2* increases mature miRNA levels and activity. **a**, **b**, Northern blotting of RNA from *let-7(n2853)* and wild-type (*N2*) worms on RNAi as indicated. The fold increase in mature miRNA normalized to tRNA levels is indicated below the relevant blots. **a**, *let-7*, *mir-77* and *mir-85*. Numbers to the right of the left blot indicate sizes in nucleotides. **b**, *mir-60*, its abundant precursor (pre-*mir-60*) and *let-7*. **c**, Pri-miRNA levels determined by RT–qPCR ($n = 3$; means ± s.e.m.). **d**, Levels of *let-7* targets *lin-41* and *daf-12* determined by RT–qPCR ($n = 3$; means ± s.e.m.). **e**, Incubation of 3′-pCp-labelled *let-7* with lysates as indicated, containing or lacking XRN-2. **f**, Incubation of 5′-end-labelled yeast $tRNA^{Phe}$ with lysate yields an array of slow-migrating bands (vertical bar) and a final product of a few nucleotides in length (arrowhead).

(Supplementary Fig. 8c), revealing the expected hydrolytic mode of degradation[20], although 3′→5′ hydrolytic exonucleases present in the lysate might have contributed to this pattern. Nuclease activity was largely sequence independent: four other synthetic miRNAs were similarly degraded (not shown). By contrast, tRNA, another small RNA with a free 3′-hydroxyl group, yielded a distinct turnover pattern (Fig. 1f). Thus, RNA structure rather than sequence might determine which RNA turnover pathway engages a given substrate in the lysate.

The exonuclease activity depended on XRN-2, because miRNA degradation was impaired with *xrn-2(RNAi)* but not *xrn-1(RNAi)* lysate (Fig. 1e and Supplementary Figs 7b and 9). Depletion of *xrn-2* was specific because the addition of bacterially expressed, recombinant glutathione *S*-transferase (GST)-tagged XRN-2 (Supplementary Fig. 10), but not GST alone, restored miRNA turnover (Fig. 1e; compare lanes 4 and 5). Consistent with the preference of 5′→3′ exoribonucleases for a 5′ phosphate on their substrates[21] was our observation that miRNA turnover was also slowed down when 5′-non-phosphorylated substrate was used (Supplementary Fig. 11). We can therefore attribute the miRNA decay activity acting in these lysates to XRN-2.

The *in vivo* assays indicated that XRN-2 affected the accumulation of the mature miRNA but not that of its precursors (Figs 1a and 2a, and Supplementary Fig. 5). To confirm this *in vitro*, we incubated radiolabelled, 5′-monophosphorylated pre-*let-7* with lysate. This substrate was converted into several products including mononucleotides (Fig. 2b), the sole product of mature miRNA turnover. When we repeated the assay with *dcr-1(RNAi)* lysate, we observed pre-*let-7* stabilization (Fig. 2c), as we did for the endogenous RNA *in vivo* (Supplementary Fig. 12). Product formation in the control lysate therefore depended on cleavage by Dicer.

In *xrn-2(RNAi)* lysate, pre-*let-7* still disappeared, which was consistent with the lack of pre-*let-7* accumulation on *xrn-2* depletion *in vivo*. However, a band migrating with a synthetic mature *let-7* accumulated in the *xrn-2(RNAi)* lysate but not in the mock RNAi lysate (Fig. 2d). We identified this band as mature *let-7* by northern analysis when performing the assay with unlabelled substrate (Fig. 2e). Pretreatment of lysates with micrococcal nuclease removed all endogenous RNA, ensuring that the mature miRNA detected by northern analysis was derived exclusively from the exogenous pre-miRNA. Micrococcal nuclease activity was terminated by the addition of

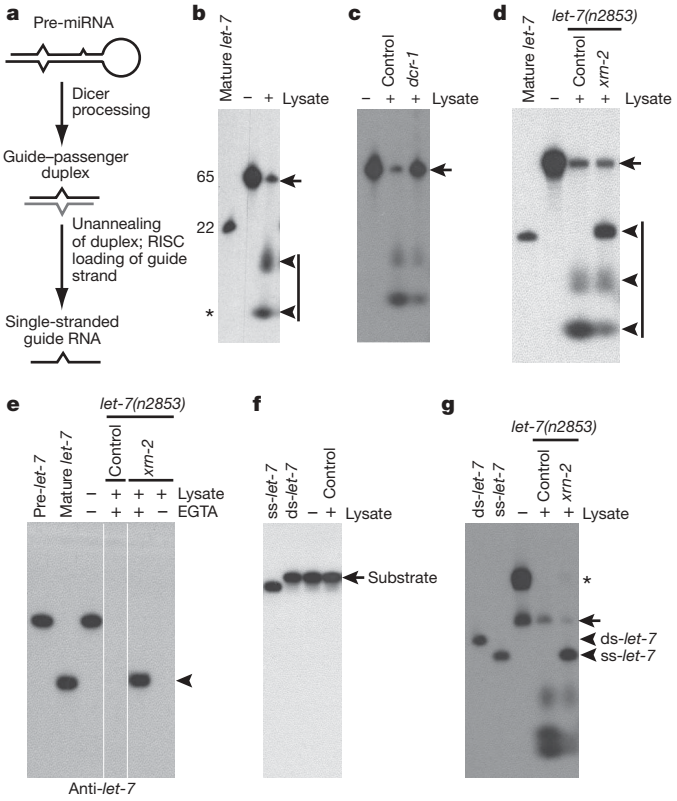

Figure 2 | Coordination of *in vitro* miRNA processing and turnover. Internally radiolabelled, 5′-monophosphorylated pre-*let-7* transcript was used unless indicated otherwise. **a**, Outline of pre-miRNA processing. **b**, Pre-*let-7* incubated with lysate. Sizes in nucleotides are indicated at the left; asterisk: gel running front. **c**, Pre-*let-7* is stabilized in *dcr-1(RNAi)* lysates. **d**, *In situ*-diced *let-7* accumulates in *xrn-2(RNAi)* lysate. **e**, Turnover of unlabelled pre-*let-7* followed by northern blotting. All lanes are from a single autoradiograph. **f**, Native gel analysis of duplex *let-7* (5′-end-labelled guide) incubated with lysate. **g**, Native gel analysis of pre *let-7* turnover products. Right asterisk, pre-*let-7* conformer; arrows, substrates; arrowheads, reaction products; ss, single-stranded; ds, double-stranded.

EGTA before the substrate was added, and no signal was detected when EGTA was omitted, confirming efficient micrococcal nuclease activity (Fig. 2e). Pre-*let-7* cleavage by Dicer is therefore a prerequisite for miRNA degradation by XRN-2. Inefficient accumulation of mature miRNA was also observed with pre-*let-7* processing in *Drosophila* embryo lysate, leading to the speculation that mature miRNA might be unstable[22]. Thus, miRNA turnover activity might be conserved in other animals.

The accumulation of an additional product about 10 nucleotides (nt) long (Fig. 2b–d and Supplementary Fig. 13) remained largely unaffected by *xrn-2(RNAi)* (Fig. 2d) but decreased on depletion of *dcr-1* (Fig. 2c) and might consist of partly degraded 'loop' RNA, generated by processing of the pre-miRNA through Dicer.

One interpretation of our results was that XRN-2 degraded the mature single-stranded miRNA in the guide–passenger RNA duplex that Dicer generates from the pre-miRNA (Fig. 2a). However, a synthetic guide–passenger duplex remained stable in lysate (Fig. 2f), suggesting that degradation should occur after separation of the two strands. Indeed, the mature *let-7* generated by pre-*let-7* processing in *xrn-2(RNAi)* lysates was single stranded, as revealed by native gel electrophoresis. (Fig. 2g). The *in vitro* system therefore recapitulates several steps in miRNA biogenesis and turnover; that is, faithful pre-miRNA processing by Dicer, unannealing of the guide–passenger duplex, and degradation of the single-stranded miRNA.

Because single-stranded miRNA was degraded whereas a guide–passenger duplex was not, we speculated that target binding might modulate miRNA stability. To test this possibility we supplemented lysates with *in vitro*-transcribed *let-7* target RNA[23]; that is, luciferase coding sequence fused to an artificial 3′ untranslated region (UTR) containing three *let-7*-binding sites or control transcripts with mutated *let-7*-binding sites or lacking the 3′ UTR entirely (Fig. 3a and Supplementary Fig. 14). Under these conditions, the transcript with *let-7*-binding sites, but not the control transcripts, stabilized the mature *let-7* miRNA produced from pre-*let-7* (Fig. 3b and Supplementary Fig. 15). The controls exclude the possibility that excess exogenous RNA simply quenched ribonuclease activity. A northern blot of an assay using unlabelled substrate confirmed mature *let-7* accumulation in the presence of target RNA (Fig. 3c). The effect was not restricted to *let-7*: identical results were obtained for pre-*mir-237* (Fig. 3d and Supplementary Figs 16 and 17). We conclude that targets can modulate the extent of mature miRNA degradation *in vitro*.

Because most cellular miRNA is thought to be associated with Argonaute proteins in the miRISC complex, we wished to confirm Argonaute-binding of the *in situ*-processed mature miRNAs. We therefore incubated radiolabelled pre-*let-7* with lysates from worms expressing green fluorescent protein (GFP)-tagged versions of both *C. elegans* miRNA argonautes, ALG-1 and ALG-2 (GFP/AGO)[24]. When GFP/AGO was subsequently immunoprecipitated from lysate lacking miRNA target, no radiolabelled RNA, precursor or mature, was co-immunoprecipitated. By contrast, addition of *let-7* target RNA to the lysate permitted the co-immunoprecipitation of mature miRNA with GFP/AGO (Fig. 3e and Supplementary Fig. 18), demonstrating incorporation into miRISC.

Depletion of *xrn-2* caused substantial accumulation of mature *let-7* from pre-*let-7* in GFP/AGO larval lysates (Fig. 3e) but permitted the co-immunoprecipitation of only modest amounts of mature *let-7* with GFP/AGO, whereas abundant *let-7* remained in the post-immunoprecipitation supernatant (Fig. 3e and Supplementary Fig. 18). We conclude that, *in vitro*, miRNAs are dislodged from ALG-1/2 through a mechanism that is efficiently modulated by the target RNA binding status of the miRNA but is only partly dependent on XRN-2. Because both the miRNA 5′ and 3′ ends are thought to be bound directly by Argonaute[25], they would be inaccessible to exoribonucleases, necessitating additional factors for release. At the same time, release and degradation steps seem to be tightly coupled *in vivo*,

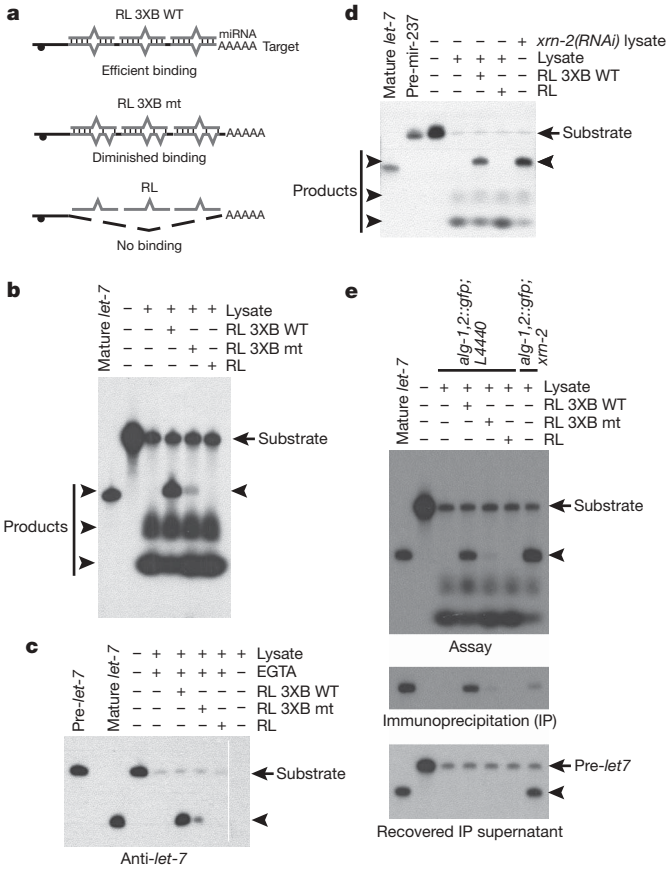

Figure 3 | Target-mediated stabilization of mature miRNA. **a**, *Renilla* luciferase reporter mRNAs with three *let-7*-binding sites (RL 3XB WT; top), three mutated sites (RL 3XB mt; middle) and lacking a 3′ UTR (RL; bottom). **b–d**, Pre-miRNA turnover using *N2* lysate in the presence of the indicated mRNAs. Substrates were radiolabelled pre-*let-7* (**b**), unlabelled pre-*let-7* analysed by northern blotting (**c**) and radiolabelled pre-*mir-237* (**d**). Right arrowheads: mature *mir-237* (23 nt) and *let-7* (22 nt). Lanes in **c** are all from a single autoradiograph. **e**, Top: pre-*let-7* turnover assay as in **b**, using *gfp::ago* lysates. Middle: mature *let-7* co-immunoprecipitated with an α-GFP antibody. Bottom: post-immunoprecipitation supernatant (separate gel).

because both *let-7* levels and activity are increased in *xrn-2(RNAi)* animals (Fig. 1, Supplementary Fig. 3 and Supplementary Table 1).

Although our data support the notion that miRNAs can be released from miRISC, this result is unexpected because human siRNA–AGO complexes are highly stable[26]. To test the stability of miRNA–AGO complexes, we immunoprecipitated GFP/AGO from larval lysate either immediately or after incubation at 25 °C. Levels of *let-7* decreased in immunoprecipitate obtained after the incubation step relative to the immunoprecipitate obtained before incubation (Fig. 4a, compare lane 1 and 2). Because the levels and integrity of GFP/AGO were unaltered, this finding supports the disassembly of the miRNA–AGO complex.

To demonstrate directly the release of AGO-bound miRNA, we immunoprecipitated GFP/AGO and incubated the protein, while bound to beads, with assay buffer with or without added KCl, or micrococcal nuclease/EGTA-treated lysates from worms exposed to mock RNAi or *xrn-2(RNAi)*. After recovery, RNA from the beads and the supernatants was probed by northern blotting for the presence of endogenous *let-7*. As expected, the addition of neither buffer nor a high concentration of salt diminished the level of AGO-bound *let-7* relative to the control, and no signal was detected in the supernatants (Fig. 4b; compare lanes 1–3). By contrast, incubation with wild-type larval lysate resulted in a strong loss of *let-7* signal from the beads and no signal in the supernatant, which is consistent with the removal of *let-7* from the ALG-1/2 complexes and its subsequent degradation (Fig. 4b, lane 4).

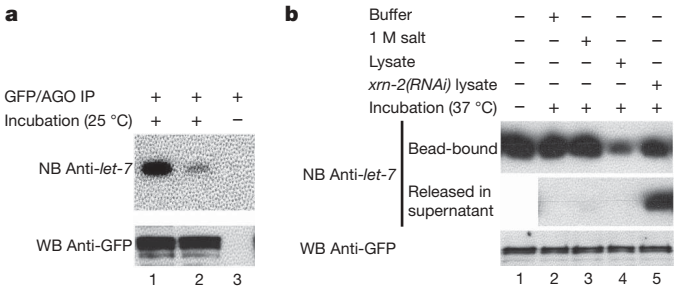

Figure 4 | Release of miRNA from miRISC. a, GFP/AGO immunoprecipitation from lysate directly or after incubation for 15 min. Half of each immunoprecipitate was subjected to northern analysis, the other half to anti-GFP western blotting. Lane 3, no antibody. **b**, Immunoprecipitated GFP/AGO proteins processed immediately (lane 1), or after incubation for 15 min with assay buffer (AB, lane 2), AB + salt (lane 3), *N2* (lane 4) or *xrn-2(RNAi)* (lane 5) lysate. RNA from supernatant and from half of the bead-bound reaction were subjected to northern analysis (top and middle, respectively). The other half of the bead-bound material was subjected to anti-GFP western blotting (bottom).

When *xrn-2*(RNAi) lysate was used to induce release, more mature miRNA remained bound to GFP/AGO (Fig. 4b; compare lanes 4 and 5), supporting a facilitating role of XRN-2 in the release process. Substantial amounts of *let-7* could be recovered in the supernatant under these conditions, confirming that efficient degradation of released miRNA depends on XRN-2.

We have shown here that XRN-2 mediates miRNA turnover *in vivo* and *in vitro*, and that it can modulate the activity of miRNAs *in vivo*. Thus, miRNA degradation contributes to miRNA homeostasis, helping to prevent detrimental overexpression of miRNAs[1]. The fact that mRNAs can stabilize their cognate miRNAs *in vitro* suggests a coordination of miRNA and target levels (Supplementary Fig. 1), permitting miRISC reprogramming when target abundance is low. When miRNA silencing is prevented or reversed[27,28], increased degradation of the concerned miRNA(s) might further enhance desilencing by preventing miRISC from target rebinding.

Although we find that XRN-2 is important in miRNA turnover *in vitro*, not all miRNAs accumulate efficiently on *xrn-2* depletion *in vivo*. It will be interesting to determine whether this reflects genuine substrate specificity or incomplete depletion of XRN-2 at times or in tissues of greatest expression of the less-affected miRNAs. It also seems likely that specialized regulatory proteins, and possibly additional ribonucleases, remain to be discovered that will guide differential turnover of individual miRNAs, for example to modulate expression profiles of specific miRNAs during developmental transitions.

METHODS SUMMARY

To prepare lysates, worms were suspended in extraction buffer (10 mM HEPES pH 7.4, 2 mM dithiothreitol (DTT), 0.1% Triton X-100, 50 mM KCl, 0.5 mM phenylmethylsulphonyl fluoride (PMSF), 10% glycerol), ground in liquid N_2 and cleared by centrifugation. RNA substrates were incubated with lysate in 1 × assay buffer (AB; 10 mM HEPES pH 7.4, 2 mM DTT, 5 mM $MgCl_2$, 100 mM KCl, 2 mM ATP).

Full Methods and any associated references are available in the online version of the paper at www.nature.com/nature.

Received 2 April; accepted 27 July 2009.
Published online 6 September 2009.

1. Chang, T. C. & Mendell, J. T. microRNAs in vertebrate physiology and human disease. *Annu. Rev. Genomics Hum. Genet.* **8,** 215–239 (2007).
2. Ding, X. C., Weiler, J. & Großhans, H. Regulating the regulators: mechanisms controlling the maturation of microRNAs. *Trends Biotechnol.* **27,** 27–36 (2009).
3. Esquela-Kerscher, A. & Slack, F. J. Oncomirs—microRNAs with a role in cancer. *Nature Rev. Cancer* **6,** 259–269 (2006).
4. Ramachandran, V. & Chen, X. Degradation of microRNAs by a family of exoribonucleases in *Arabidopsis*. *Science* **321,** 1490–1492 (2008).
5. Büssing, I., Slack, F. J. & Großhans, H. *let-7* microRNAs in development, stem cells and cancer. *Trends Mol. Med.* **14,** 400–409 (2008).
6. Reinhart, B. J. *et al.* The 21-nucleotide *let-7* RNA regulates developmental timing in *Caenorhabditis elegans*. *Nature* **403,** 901–906 (2000).
7. Vella, M. C., Choi, E. Y., Lin, S. Y., Reinert, K. & Slack, F. J. The *C. elegans* microRNA *let-7* binds to imperfect *let-7* complementary sites from the *lin-41* 3′UTR. *Genes Dev.* **18,** 132–137 (2004).
8. Bagga, S. *et al.* Regulation by *let-7* and *lin-4* miRNAs results in target mRNA degradation. *Cell* **122,** 553–563 (2005).
9. Abbott, A. L. *et al.* The *let-7* microRNA family members *mir-48*, *mir-84*, and *mir-241* function together to regulate developmental timing in *Caenorhabditis elegans*. *Dev. Cell* **9,** 403–414 (2005).
10. Kennedy, S., Wang, D. & Ruvkun, G. A conserved siRNA-degrading RNase negatively regulates RNA interference in *C. elegans*. *Nature* **427,** 645–649 (2004).
11. Chernyakov, I., Whipple, J. M., Kotelawala, L., Grayhack, E. J. & Phizicky, E. M. Degradation of several hypomodified mature tRNA species in *Saccharomyces cerevisiae* is mediated by Met22 and the 5′–3′ exonucleases Rat1 and Xrn1. *Genes Dev.* **22,** 1369–1380 (2008).
12. Weidhaas, J. B. *et al.* MicroRNAs as potential agents to alter resistance to cytotoxic anticancer therapy. *Cancer Res.* **67,** 11111–11116 (2007).
13. Gy, I. *et al. Arabidopsis* FIERY1, XRN2, and XRN3 are endogenous RNA silencing suppressors. *Plant Cell* **19,** 3451–3461 (2007).
14. Lee, R. C. & Ambros, V. An extensive class of small RNAs in *Caenorhabditis elegans*. *Science* **294,** 862–864 (2001).
15. Ketting, R. F. *et al.* Dicer functions in RNA interference and in synthesis of small RNA involved in developmental timing in *C. elegans*. *Genes Dev.* **15,** 2654–2659 (2001).
16. Grishok, A. *et al.* Genes and mechanisms related to RNA interference regulate expression of the small temporal RNAs that control *C. elegans* developmental timing. *Cell* **106,** 23–34 (2001).
17. Großhans, H., Johnson, T., Reinert, K. L., Gerstein, M. & Slack, F. J. The temporal patterning microRNA *let-7* regulates several transcription factors at the larval to adult transition in *C. elegans*. *Dev. Cell* **8,** 321–330 (2005).
18. Slack, F. J. *et al.* The *lin-41* RBCC gene acts in the *C. elegans* heterochronic pathway between the *let-7* regulatory RNA and the LIN-29 transcription factor. *Mol. Cell* **5,** 659–669 (2000).
19. Ding, X. C. & Großhans, H. Repression of *C. elegans* microRNA targets at the initiation level of translation requires GW182 proteins. *EMBO J.* **28,** 213–222 (2009).
20. Stevens, A. & Poole, T. L. 5′-exonuclease-2 of *Saccharomyces cerevisiae*. Purification and features of ribonuclease activity with comparison to 5′-exonuclease-1. *J. Biol. Chem.* **270,** 16063–16069 (1995).
21. Stevens, A. & Maupin, M. K. A 5′–3′ exoribonuclease of human placental nuclei: purification and substrate specificity. *Nucleic Acids Res.* **15,** 695–708 (1987).
22. Hutvagner, G. *et al.* A cellular function for the RNA-interference enzyme Dicer in the maturation of the *let-7* small temporal RNA. *Science* **293,** 834–838 (2001).
23. Pillai, R. S. *et al.* Inhibition of translational initiation by let-7 microRNA in human cells. *Science* **309,** 1573–1576 (2005).
24. Hutvagner, G., Simard, M. J., Mello, C. C. & Zamore, P. D. Sequence-specific inhibition of small RNA function. *PLoS Biol.* **2,** E98 (2004).
25. Wang, Y., Sheng, G., Juranek, S., Tuschl, T. & Patel, D. J. Structure of the guide-strand-containing argonaute silencing complex. *Nature* **456,** 209–213 (2008).
26. Martinez, J. & Tuschl, T. RISC is a 5′ phosphomonoester-producing RNA endonuclease. *Genes Dev.* **18,** 975–980 (2004).
27. Bhattacharyya, S. N., Habermacher, R., Martine, U., Closs, E. I. & Filipowicz, W. Relief of microRNA-mediated translational repression in human cells subjected to stress. *Cell* **125,** 1111–1124 (2006).
28. Kedde, M. *et al.* RNA-binding protein Dnd1 inhibits microRNA access to target mRNA. *Cell* **131,** 1273–1286 (2007).

Supplementary Information is linked to the online version of the paper at www.nature.com/nature.

Acknowledgements We thank M. Bühler and W. Filipowicz for critical comments on the manuscript; W. Filipowicz for plasmids; C. Mello and F. Slack for *C. elegans* strains; and A. Esquela-Kerscher for sharing Starfire probes for pre-miRNA detection. S.C. was supported by Marie Curie and EMBO long-term postdoctoral fellowships.

Author Contributions S.C. and H.G. designed the research. S.C. designed and performed the experiments. S.C. and H.G. analysed the experimental results and wrote the manuscript.

Author Information Reprints and permissions information is available at www.nature.com/reprints. Correspondence and requests for materials should be addressed to H.G. (helge.grosshans@fmi.ch).

METHODS

Worm strains, *let-7(n2853)* suppression and RNAi. The wild-type strain was *C. elegans* var. Bristol strain *N2*. The other two strains were *let-7(n2853)* (ref. 6) and *gfp::alg-1;gfp::alg-2* (ref. 24). Suppressors of *let-7(n2853)* were identified by RNAi by feeding growing worms on RNAi plates at 25 °C as described[17,29].

RNA isolation, northern blotting and RT–qPCR. Total RNA was isolated from staged L4 worms, unless indicated otherwise, that were frozen in liquid nitrogen and ground in a mortar, using the Trizol (Invitrogen) method in accordance with the manufacturer's instruction. Northern blotting of endogenous RNA was performed as described[30]. 5′-labelled (using T4 polynucleotide kinase (PNK) and [γ-^{32}P]ATP) DNA oligos were used as probes except for those in Supplementary Fig. 5, in which STARFIRE probes were used. The hybridization for *let-7* miRNA was conducted at an elevated temperature of 40 °C to minimize the binding of the probe to *let-7* sisters. For northern analysis of *in vitro* turnover assay products, the lysates were pretreated with micrococcal nuclease (NEB; 0.5–1.0 μl per 100 μg of lysate) for 10 min at 37 °C followed by the addition of EGTA to a final concentration of 7.5 mM. Pretreatment with micrococcal nuclease was done to digest all endogenous RNAs from the lysates, ruling out the possibility of detection of endogenous RNA. Excess EGTA was used to terminate the micrococcal nuclease treatment. '−EGTA' lysate served as a positive control for micrococcal nuclease activity that removed all the RNA, including exogenous RNA, resulting in no signal. After incubation of RNAs in the lysates, the samples were extracted with phenol/chloroform and precipitated with alcohol. The recovered samples were subjected to northern probing using the conditions stated above. RT–qPCR was performed as described[19].

Cloning and expression of recombinant XRN-2. *xrn-2* complementary DNA was amplified from total RNA by RT–PCR, and cloned in a TOPO TA vector (Invitrogen). The sequence-confirmed correct ORF was subcloned in pGEX 4T-1 (GE Healthcare) and expressed in *Escherichia coli* as a GST fusion protein. The recombinant protein was extracted with detergent from inclusion bodies and then resolved by SDS–PAGE. After KCl staining[31], the band of pure recombinant protein was excised and the protein was eluted with buffer PEB (0.05 M Tris-HCl pH 8.0, 0.2 M NaCl, 0.1 mM EDTA, 5 mM DTT, 0.2% SDS) overnight at 37 °C. The eluate was stored in aliquots at −80 °C. Before use, the recombinant protein was refolded by diluting 1:20 in TETN 250 buffer containing 0.1% Triton X 100 (ref. 32), and incubated for 2 h at 4 °C. Finally the protein was concentrated with Microcon-100 (Millipore) and its concentration was estimated with a Bradford assay (Bio-Rad). The use of gel-purified and renatured GST–XRN-2 (about 140 kDa) essentially eliminated any possibility of contamination by 5′→3′ exoribonuclease activity of bacterial origin because proteins larger than 100 kDa are rare in *E. coli*. Moreover, bacterial cells are thought to be largely devoid of endogenous 5′→3′ exoribonucleases, with the only known bacterial activity residing in a 66-kDa protein, the *B. subtilis* endoribonuclease/exoribonuclease ribonuclease J1 (ref. 33).

Preparation of RNA substrates. Pre-*let-7*/pre-*mir-237* or mature *let-7* RNA were prepared essentially by following the methods described elsewhere[34]. In brief, a chimaeric RNA containing in its 5′ portion a hammerhead ribozyme followed by the pre *let-7*/mature *let-7* sequence was transcribed from DNA cassettes with a T7 MAXIscript kit (Ambion) in the presence of [α-^{32}P]UTP or unlabelled UTP. The DNA cassettes were prepared by the annealing of appropriate forward and reverse primers (see the oligo sequence section) followed by Klenow fill-in reactions. Double-stranded DNAs of appropriate lengths were gel-purified and amplified by PCR (except pre-*miR-237* and mature *let-7*, which were directly used as transcription substrate after gel purification) with appropriate flanking primers. Gel-purified PCR products were used as the templates for *in vitro* transcription reactions. Moreover, before use, the PCR products were cloned and their sequences were confirmed. Self-processing of the ribozyme-containing transcripts occurred during the course of transcription reaction. The resulting pre-*let-7*/mature *let-7*, which contained 5′ hydroxyl groups, were size-purified with 8–10% PAGE in the presence of 7 M urea. After recovery, RNAs were 5′ phosphorylated with T4 PNK and ATP. Before use the pre-*let-7* RNA was subjected to refolding as described[34].

5′ labelling of synthetic mature miRNAs and tRNA (after dephosphorylation; yeast tRNA^{Phe}; Sigma) was performed with PNK and [γ-^{32}P]ATP. 3′ labelling and blocking of synthetic mature miRNAs were performed with T4 RNA ligase and [5′-^{32}P]pCp, in accordance with the manufacturer's instructions (Ambion). All RNAs were gel purified.

The 5′-7-methyl-G-capped RL reporter mRNAs[23] (*Renilla* luciferase with an artificial 3′ UTR harbouring 3X bulged *let-7*/*mir-237* complementary sites (RL 3XB WT), *Renilla* luciferase followed by mutated 3X bulged *let-7* complementary sites (RL 3XB mt), and *Renilla* luciferase without 3′ UTR (RL)) were prepared by *in vitro* run-off transcription of appropriately digested plasmids using standard reagents from a T7 MEGAscript kit and cap analogue m^{7}G(5′)ppp(5′)G from Ambion, in accordance with the manufacturer's instructions. After extraction with phenol/chloroform and precipitation with alcohol, the RNAs were polyadenylated with *E. coli* PolyA polymerase (Stratagene) and ATP.

The construct for RL mRNA with an artificial 3′ UTR harbouring 3X bulged *mir-237* target sites were prepared by swapping the bulged *let-7* complementary sites in the pRL 3XB WT vector[23] with bulged *miR-237* complementary sites.

Preparation of worm lysate. Staged L4 worms grown on plates were harvested with M9 buffer (22 mM KH_2PO_4, 22 mM Na_2HPO_4, 85 mM NaCl, 1 mM $MgSO_4$) and washed three times with the same buffer. The worm pellet was then resuspended in extraction buffer (10 mM HEPES pH 7.4, 2 mM DTT, 0.1% Triton X-100, 50 mM KCl, 0.5 mM PMSF, 10% glycerol) and ground in liquid N_2. After thawing, the sample was centrifuged at 14,000*g* or more for 15–20 min; the clear supernatant was collected and designated as cleared worm lysate.

***In vitro* turnover assay.** Labelled RNAs (pre-*let-7*/pre-*mir-237* and mature *let-7*, about 1 and 2 fmol, respectively) were incubated for 15 min with cleared worm lysate (2–20 μg) in 1 × assay buffer (AB; 10 mM HEPES pH 7.4, 2 mM DTT, 5 mM $MgCl_2$, 100 mM KCl, 2 mM ATP) in a volume of 10 μl at 25 or 37 °C. The reactions were stopped by addition of 1 volume of formamide gel loading buffer (95% formamide, 0.2% SDS, 1 mM EDTA, 0.04% xylene cyanol, 0.04% bromophenol blue) followed by heating at 65 °C for 5 min. Equal volumes of the samples were then subjected to 8–12% PAGE in the presence of 7 M urea, followed by gel drying and autoradiography or phosphorimaging.

The target-mRNA-mediated miRNA stabilization assays were performed with 1 fmol of radiolabelled substrate and 20 fmol of the concerned target mRNA in volumes of 20 μl.

For add-back assays, the *xrn-2(RNAi)* lysate was preincubated with the recombinant protein (about 7 ng per reaction) on ice for 30 min to achieve reconstitution, and then used for the assay.

For native gel analysis of pre-*let-7* assay products, reactions were performed as above except that after incubation the samples were subjected to treatment with proteinase K (PK) as described[35] at 20–23 °C for 30 min, and then resolved in a 15% native polyacrylamide gel at 4 °C, using a native gel loading buffer[35].

Guide–passenger duplex with a 5′-^{32}P-labelled guide strand was prepared using methods described previously[35]; 10,000 c.p.m. of the native gel purified substrate was used in each reaction. After incubation with lysate, analysis of the sample was performed under native conditions as for pre-*let-7* (above).

Coupled pre-*let-7* processing and Ago immunoprecipitation. Pre-*let-7* assay was performed as described above in the absence or presence of target mRNA, using a lysate obtained from a strain in which both the *C. elegans* miRISC Argonaute proteins ALG-1 and ALG-2 were tagged with GFP ('GFP/AGO'; ref. 24). After incubation for 15 min at 37 °C, the reaction volumes were increased to 200 μl with 1 × AB and subjected to immunoprecipitation at 4 °C for 2 h with an anti-GFP antibody (anti-GFP mouse IgG; monoclonal antibody, catalogue no. 11 814 460 001; Roche) and Protein A-Sepharose CL-4B (GE Healthcare). The recovered Sepharose beads were suspended in formamide gel loading buffer, heated at 65 °C for 5 min and centrifuged briefly; the supernatants were subjected to urea-PAGE analysis. The post-immunoprecipitate supernatants were also recovered through phenol/chloroform extraction and alcohol precipitation, and subjected to urea-PAGE analysis.

Thin-layer chromatography. Mature miRNA turnover reactions using [α-^{32}P]UTP-labelled miRNA were stopped by the addition of SDS to 1% concentration and EDTA to 10 mM. Aliquots of 1 μl were spotted onto prewashed PEI-cellulose plates (Macherey-Nagel) and developed sequentially with 0.5 M LiCl and 1 M formic acid[36]. Unlabelled uridine 5′-monophosphate and uridine 5′-diphosphate were also separated on the same plate and detected through fluorescence quenching.

miRNA release assay. Immunoprecipitation of GFP-tagged ALG-1/ALG-2 complexes was performed essentially by following the methods described elsewhere[37] with the aforementioned anti-GFP antibody. The bead-bound immunoprecipitates (derivative of 400 μg of lysate protein per reaction) were incubated with 1 × AB, 1 × AB plus KCl (to a final concentration of about 1.0 M) or 100 μg of micrococcal nuclease/EGTA-treated empty vector and *xrn-2(RNAi)* lysate, at 37 °C for 15 min. After further recovery the beads were split into two halves. RNA was extracted from one half for northern analysis; the other half was boiled in SDS sample buffer and subjected to SDS–PAGE and western blotting with a rabbit polyclonal anti-GFP antibody (ab6556-25; Abcam), to confirm equal binding of AGO to the beads and integrity of the proteins. RNA was also extracted from the above supernatant fractions (not split) and subjected to northern analysis to detect miRNAs released in the supernatant.

In the parallel approach, immunoprecipitation was performed from lysate before and after incubation at the worm's physiological temperature (25 °C) for 15 min, and the immunoprecipitate was subjected to both northern and western probing as mentioned above.

Oligos (5′-3′). Northern: *let-7(WT)*, 5′-AAC TAT ACA ACC TAC TAC CTC A-3′; *let-7(n2853)*, 5′-AAC TAT ACA ACC TAC TAT CTC A-3′; *mir-77*, 5′-TG G ACA GCT ATG GCC TGA TGA A-3′; *mir-85*, 5′-GCA CGA CTT TTC AAA TAC TTT GTA-3′; *pre mir-60*, 5′-CT TGA ACT AGA AAA TGT GCA TAA TA TCA CGT ACT TTG TCA TG-3′; $tRNA^{Gly}$, 5′-GCTTGGAAGGCATCCATG CTGACCATT-3′. STARFIRE probes (IDT) against the following miRNAs were used: *let-7*, *mir-237*, *lin-4*, *mir-34*, *mir-240*, *mir-75*, *mir-245*, *mir-234*, *mir-79*, *mir-84*, *mir-48*, *mir-85*.

qPCR: primary *let-7*, 5′-TCCTAGAACACATCTCCCTTTGA-3′ (forward) and 5′-CGCAGCTTCGAAGAGTTCTG-3′ (reverse); primary *mir-77*, 5′-CATT GTTCGTTTCGCTTTCA-3′ (forward) and 5′-CCAATAACTGATTCAACATT CCAA-3′ (reverse); *daf-12* mRNA, 5′-GAT CCT CCG ATG AAC GAA AA-3′ (forward) and 5′-CTC TTC GGC TTC ACC AGA AC-3′ (reverse); *lin-41* mRNA, 5′-GGA TTG TTC GAC ACC AAC G-3′ (forward) and 5′-ACC ATG ATG TCA AAC TGC TGT C-3′ (reverse); *xrn-2* mRNA, 5′-GATCCCGAGTACCCA CAAGA-3′ (forward) and 5′-CCACCACCACCTCTCACATA-3′ (reverse).

Cloning: *xrn-2* cDNA, 5′-GAAA GAATTC ATG GGA GTT CCC GCA TTC TTC AG-3′ (forward primer) and 5′-GAAA GCGGCCGC GAT TAT CTC CAT GAT GAA TTT CCG TG-3′ (reverse primer). 3X *mir-237* target cassette construction: template sequence, 5′-GGGG tctaga AGC TGT TCG AGA ATT TTGAA CTC AGG GA ctcggagc AGC TGT TCG AGA ATT TTGAA CTC AGG GA ctcggagc AGC TGT TCG AGA ATT TTGAA CTC AGG GA gcggccgc AAAG-3′. Primers for PCR amplification of 3X mir-237 target cassette: 5′-GGG GTC TAG AAG CTG TTC GAG AAT TTT G-3′ (forward primer) and 5′-CTT TGC GGC CGC TCC CTG AGT TCA AAA TTC-3′ (reverse primer).

Preparation of templates for *in vitro* transcription: mature *let-7* cassette, 5′-G TAA TAC GAC TCA CTA TAG GGAGA CTA CTA CCT CAC TGA TGA GTC CGT GAG GAC GAA ACG GTA CCC GGT ACC GTC TGA GGT AGT AGG-3′ (forward primer (T7 promoter, HH ribozyme, first 12 *let-7* nucleotides)) and 5′-AAC TAT ACA ACC TAC TAC CTC A GAC GGT ACC GGG-3′ (reverse primer (mature *let-7* complementary sequence, 12 nucleotides; complementary region to HH ribozyme)). *Pre-let-7* cassette: 5′-G TAA TAC GAC TCA CTA TAG GGAGA CTA CTA CCT CAC TGA TGA GTC CGT GAG GAC GAA ACG GTA CCC GGT ACC GTC TGA GGT AGT AGG-3′ (forward primer (T7 promoter, HH ribozyme, first 12 *let-7* nucleotides)) and 5′-GGT AAG GTA GAA AAT TGC ATA GTT CAC CGG TGG TAA TAT TCC AAA CTA TAC AAC CTA CTA CCT CA GAC GGT ACC GGG-3′ (reverse primer (pre-*let-7* complementary sequence, 12 nucleotides; complementary region to HH ribozyme)). Primers for PCR amplification of mature *let-7* cassette: 5′-GAATTC TAA TAC GAC TCA CTA TAG G-3′ (forward T7 promoter primer) and 5′-AAC TAT ACA ACC TAC TAC CTC A-3′ (*let-7* guide reverse primer). Primers for PCR amplification of pre-*let-7* cassette: 5′-GAATTC TAA TAC GAC TCA CTA TAG G-3′ (forward T7 promoter primer) and 5′-GGT AAG GTA GAA AAT TGC ATA G-3′ (*let-7* passenger reverse primer). Pre-*mir-237* cassette: 5′-G TAA TAC GAC TCA CTA TAG GGAGA GAA TTC TCA GGG A C TGA TGA GTC CGT GAG GAC GAA ACG GTA CCC GGT ACC GTC TCC CTG AGA ATT C-3′ (forward primer (T7 promoter, HH ribozyme, first 13 *mir-237* nucleotides)) and 5′-GGT CCT TGA CAA AAC TCG ACA GCT TGA ACA CTT TGA AGC TGT TCG AGA ATT CTC AGG GAGAC GGT ACC GGG-3′ (reverse primer (pre-*mir-237* complementary sequence, 12 nucleotides; complementary region to HH ribozyme)).

29. Ding, X. C., Slack, F. J. & Großhans, H. The let-7 microRNA interfaces extensively with the translation machinery to regulate cell differentiation. *Cell Cycle* **7,** 3083–3090 (2008).
30. Pall, G. S. & Hamilton, A. J. Improved northern blot method for enhanced detection of small RNA. *Nature Protocols* **3,** 1077–1084 (2008).
31. Hager, D. A. & Burgess, R. R. Elution of proteins from sodium dodecyl sulfate-polyacrylamide gels, removal of sodium dodecyl sulfate, and renaturation of enzymatic activity: results with sigma subunit of *Escherichia coli* RNA polymerase, wheat germ DNA topoisomerase, and other enzymes. *Anal. Biochem.* **109,** 76–86 (1980).
32. Chatterjee, S. *et al.* An RNA-binding respiratory component mediates import of type II tRNAs into *Leishmania* mitochondria. *J. Biol. Chem.* **281,** 25270–25277 (2006).
33. Mathy, N. *et al.* 5′-to-3′ exoribonuclease activity in bacteria: role of RNase J1 in rRNA maturation and 5′ stability of mRNA. *Cell* **129,** 681–692 (2007).
34. Kolb, F. A. *et al.* Human dicer: purification, properties, and interaction with PAZ PIWI domain proteins. *Methods Enzymol.* **392,** 316–336 (2005).
35. Matranga, C., Tomari, Y., Shin, C., Bartel, D. P. & Zamore, P. D. Passenger-strand cleavage facilitates assembly of siRNA into Ago2-containing RNAi enzyme complexes. *Cell* **123,** 607–620 (2005).
36. Dziembowski, A., Lorentzen, E., Conti, E. & Séraphin, B. A single subunit, Dis3, is essentially responsible for yeast exosome core activity. *Nature Struct. Mol. Biol.* **14,** 15–22 (2007).
37. Lee, M. H. & Schedl, T. Identification of *in vivo* mRNA targets of GLD-1, a maxi-KH motif containing protein required for *C. elegans* germ cell development. *Genes Dev.* **15,** 2408–2420 (2001).